Journal of Thermal Analysis, Vol. 30 (1985) 1035–1045

EFFECT OF TEMPERATURE AND ^{60}Co γ-RADIATION DAMAGE ON THE ELECTRICAL AND STRUCTURAL PROPERTIES OF $BaZrO_3$ CERAMICS

A. Tawfik, M. I. Ab'd El-Ati and F. M. El-Ashry

FACULTY OF SCIENCE, TANTA UNIVERSITY, TANTA, EGYPT

(Received November 5, 1984; in revised form March 27, 1985)

Well-sintered barium zirconate ceramic bodies have been prepared and identified. Extensive measurements have been made on these specimens, including X-ray diffraction, and DC-electrical conductivity as a function of temperature before and after exposure to a gamma-radiation dose and after various periods (radiation decay time) following removal of the specimens, from the radiation field. The resistivity *vs.* temperature curve showed an abrupt change at around 60°, in the reverse direction, indicative of a probable transition from an *n*- to a *p*-type semiconduction mechanism. Finally, all the results are discussed in detail and correlated on the basis of the interactions of temperature, ionizing radiation damage and radiation annihilation with the barium zirconate lattice.

$BaZrO_3$ has a cubic perovskite lattice structure [1–3]. The small Zr cation (radius 0.87 Å) is surrounded by six oxygen anions (radius 1.32 Å); the Ba cations (radius 1.43 Å), occupy the corners of a cube. The principal method adopted for preparing polycrystalline ceramic samples is by sintering [4–6]. $BaZrO_3$ is normally a *p*-type semiconductor [7], and its volume resistivity is linear.

A temporary change in electrical conductivity is induced when ionizing radiation is absorbed in solid materials by the production of electrons or "positive holes" having sufficient energy to be free to move through the solid. This "induced conductivity" is a function of the absorbed dose rate in the material and can be used as a measure of the dose rate or exposure rate if appropriate calibrations are made [8]. In certain materials a permanent change in conductivity may be produced by radiation damage to the crystal; in these materials, the change is a function of the total dose absorbed in the material. The chief advantage of solid-state conductivity devices is that their high density and low ionization potential enable dosimeters of small volume to be constructed.

If a DC voltage is applied to *p-n* junctions or to other photoconductors, a current will be measured as a function of the dose absorbed in, or exposure rate at, the photoconductor.

John Wiley & Sons, Limited, Chichester
Akadémiai Kiadó, Budapest

The photovoltage or photocurrent will be a function of the absorbed dose rate in the detector. The change in conductivity is transistory, and the substance is assumed to return to its original state after the irradiation, with a time constant depending upon the electronic properties of the material. However, if the structure of the solid is altered permanently, e.g. by a large dose of γ-rays or a moderate dose of neutrons, the electrical conductivity in the absence of radiation may be changed permanently [9]. This change in conductivity can be measured as a function of the absorbed dose in the detector, so that the system is then an integrating dosimeter.

In the present manuscript, constant irradiation of the material was selected in order to produce a constant induced current when voltage is applied which must be biased off. This treatment was based on previous deductions [10, 11] and is called biasing, and the constant current is comparable to the signal current to be measured.

The present investigation was carried out in an attempt to throw light on the effects of ionizing radiation on the structural and electrical properties, including the mobility of current carriers, and to understand if possible the mechanism of interaction of the ionizing radiation with the $BaZrO_3$ lattice.

Experimental

A) Synthesis and sample preparation

Using a high-speed mixer for 4 hr, $BaZrO_3$ was prepared by mixing pure finely powdered $BaCO_3$ with ZrO_2 in equimolar amounts. The mixture was dried at 150° and pulverized in an agate morter. The dried mixture was then fired at 1200° in an alumina crucible in a normal atmosphere for 2 hr. These conditions followed the usual ceramic technique and firing procedure for obtaining $BaZrO_3$. A few of distilled water were added to the powder as a binder and tablets 1.5 cm in diameter and 0.1 cm thick were pressed at about 5 kg/cm^2 The pressed tablets were then sintered at 1400° in a muffle furnace for 3 hr at atmospheric pressure, and were allowed to cool down to room temperature in 24 hr. The tablets were polished, and painted on both flat surface with silver paste. In this respect, silver paste diffusion or its troubles on connecting electrodes were negligible here, due to the relatively moderate temperature of measurements ($<170°$), while evaporated Pt-electrodes were used. The starting materials used in the preparation were analytically pure reagents (BDH, 99.8%). Some of the tablets were exposed to ^{60}Co γ-irradiation at a dose of 1.8×10^5 rad.

B) Identification of the prepared material

X-ray diffraction patterns of $BaZrO_3$ and its irradiation samples were recorded with a Shimadou (Japan) X-ray diffractometer. Cu—K_α radiation and a nickel filter were used. The Bragg angle, $2\theta°$, the corresponding d spacings and the relative intensities of the diffraction peaks were evaluated together with the corresponding values in the A.S.T.M. index for $BaZrO_3$ ceramic.

C) Measurements of the DC electrical resistivity and current (I) as functions of temperature

In the present work, the sample was connected to an RM 290 megaohmeter, and the resistivity was determined from the relation:

$$\varrho = R\frac{A}{d} \tag{1}$$

where d is the sample thickness and A its cross-sectional area (cm^2). The circuit used was very similar to that described previously [6].

The electrical resistivity values were taken 15 min after each temperature equilibration in the temperature range 312–434 K. The readings were checked twice for every 5 degrees of temperature.

The absorption current appeared after a long time and for this reason the d.c. voltage was applied for 24 hr before measurements. The temperature was raised by an electric furnace, and was measured with a Cu/Cu-constantan thermocouple and a temperature relay technique.

D) Gamma radiation exposure

Barium zirconate ceramic pellets were exposed to ^{60}Co γ-rays at an absorbed dose of 1.8×10^5 rad in air at the Egyptian Atomic Energy Establishment (AEE).

All measurements were performed before and after the absorbed gamma-radiation dose, as well as after removal of the specimens from the radiation field.

Results and discussion

Figure 1 shows the X-ray diffraction patterns of $BaZrO_3$ (B) before irradiation and (A) after irradiation.

The values of the interplanar spacings (d) of the hkl planes and the relative intensities (I/I_0) for each line were evaluated. Table 1 presents their analysis for each diffraction peak before the absorbed gamma dose (pattern B) and after irradiation (pattern A). Comparing and matching of the results obtained with those given by earlier authors [1–3] confirmed a cubic perovskite structure for the present $BaZrO_3$.

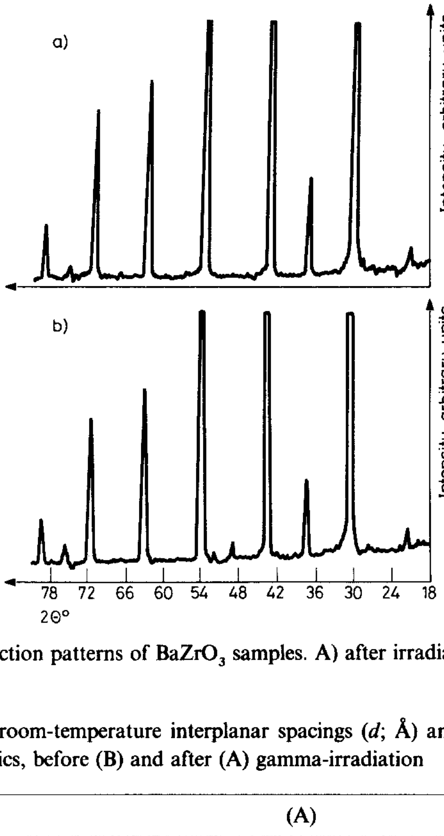

Fig. 1 X-ray diffraction patterns of $BaZrO_3$ samples. A) after irradiation, B) before irradiation

Table 1 Values of the room-temperature interplanar spacings (d; Å) and relative intensities (I/I_0) of $BaZrO_3$ ceramics, before (B) and after (A) gamma-irradiation

(B)			(A)			A.S.T.M.	
2Θ	d, Å	I/I_0	2Θ	d, Å	I/I_0	d, Å	I/I_0
21° 25′	4.1795	4	21° 25′	4.1795	4	4.194	10
30° 60′	2.9190	100	29° 00′	3.0769	2	2.965	100
37° 20′	2.4149	11	30° 25′	2.9515	100	2.421	9
43° 25′	2.0906	60	37° 25′	2.4124	14	2.097	34
48° 65′	1.8703	3	43° 30′	2.0878	80	1.875	2
51° 65′	1.7681	2	53° 65′	1.7079	59	1.7116	37
53° 80′	1.7025	66	62° 80′	1.4784	29	1.4824	19
62° 80′	1.4375	27	71° 20′	1.3232	25	1.3258	17
71° 20′	1.3232	22	73° 30′	1.2904	2	1.2641	2
75° 30′	1.2610	3	79° 30′	1.2071	8	1.1206	16
79° 30′	1.2071	6				1.0482	3

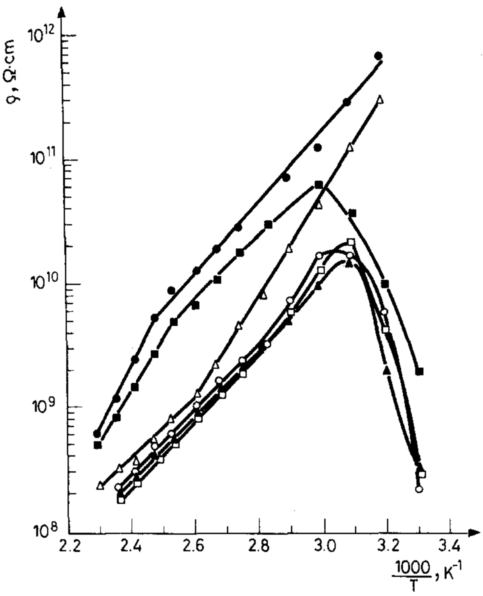

Fig. 2 Dependence of log resistivity (ϱ) on the inverse absolute temperature for samples (●) before irradiation, ■) 9 days, △) 19 days. ○) 23 days, ▲) 25 days, □) 28 days after gamma-irradiation

After the absorbed gamma dose (pattern A), the X-ray diffractograms display a slightly decreased degree of crystallinity, indicating a slight shift to the amorphous phase [12]. This could be explained by the direct action of the absorbed dose in the formation of decomposition product and melting of the material by the energetic gamma-rays, producing a glassy phase incorporated within the crystalline matrix.

Furher, comparison of the interplanar spacings and relative intensities deduced from the X-ray diffraction pattern with those of the A.S.T.M. index confirms $BaZrO_3$ in the perovskite cubic phase as starting material. The X-ray diffraction pattern of the irradiated sample shows the disappearance of some lines, which confirms the change of the cubic structure to pseudo-cubic. This confirms the migrations of the Zr ions from their rest positions to interstitial lattice sites and/or partial decomposition of barium zirconate to zirconia and baria. Thus, when $BaZrO_3$ ceramic tablets are exposed to γ-radiation, the excited Zr ions may leave their positions, as confirmed by the X-ray lattice distortion (Fig. 1). These vacancies cause an increase in the mobility of charge carriers. Zr^{4+} leaves its initial position as time passes. This increases the number of vacancies through the lattice of radiated $BaZrO_3$, giving rise to induced mobility and conductivity.

In Fig. 2, the increase of resistivity with temperature below 60° and its subsequent decrease with temperature above 60°, is most probably correlated with the conversion from a p- to an n-type conduction mechanism through Zr vacancies. This is because Zr occupies the B position in the formula ABO_3 and this small ion is surrounded by six larger oxygen anions, while the even larger Ba cations occupy the corners of the cube.

The formation of the above-mentioned glassy phase is reflected in the increased electrical conductivity and its attendant decreased activation energy for conduction after irradiation (Fig. 2). Further, as a result of the absorbed gamma-radiation dose, the following effects could be detected (see X-ray diffraction patterns A and B in Fig. 1):

a) Some peaks completely disappear (at $2\theta = 48.65$ and 52°). This could be ascribed to the decreased degree of crystallinity and partial formation of the glassy phase.

b) Other peaks are newly created (at $2\theta = 20°$ and 29°) and this is most probably correlated with the formation of decomposition products as a result of γ-radiation damage. The decomposition products are plausibly expected to be ZrO_2 and BaO, according to the radiolytic decomposition:

$$nBaZrO_3 \rightarrow (n-x)BaZrO_3 + xZrO_2 + xBaO \ldots \quad (2)$$

where x means minute traces, depending on the gamma-ray dose energy.

Since the interplanar spacings and relative intensities remain nearly unchanged after irradiation, we can say that the radiation damage cannot affect the lattice transformation in the dose range utilized.

Thus, the increased electrical conductivity after irradiation supports the idea that the irradiation introduced lattice defects [13, 14] which may lead to donor centres (Fig. 2).

In accordance with Smith [15], the lattice damage caused by gamma-radiation in the present semiconducting material does not generally alter the lattice parameters, bonding length, effective mass or overall band structure, but damage is accompanied primarily by vacancies and interstitial atoms which lead to additional energy levels.

In the low-temperature region, some samples demonstrate a negative temperature-dependence of the electrical conductivity. This is most probably correlated with gamma-radiation-induced polarization and accumulation of charges at the surface of the specimens (as caused by radiation-induced atomic displacement). A further contribution to the increased electrical conductivity is an enhancement of the diffusion of Ba and Zr impurities in the $BaZrO_3$ lattice by gamma-irradiation [6].

It must be noted that, after the material is removed from the radiation field, the radiation-induced electrical conductivity (Fig. 2) and radiation-induced current (Fig. 3) fall. This could be ascribed to radiation "annihilation" leaving behind radiation damage [17].

Figures 4 and 5 show the variation in the activation energy for conduction (eV) and the mobility of the charge carrier (cm^2 V^{-1} s^{-1}), respectively, as a function of the decay time (the time after removal of the material from the radiation field). The two relations (Figs 4 and 5) are in conformity. The current at low field (Fig. 3) varies with temperature in accordance with the following equation:

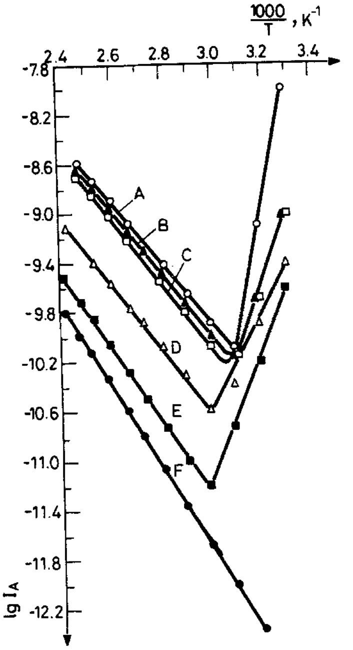

Fig. 3 Relation between log I_A and $\frac{1000}{T}$ K^{-1} A) 28 days, B) 25 days, C) 23 days, D) 19 days, E) 9 days after gamma-irradiation, F) before irradiation

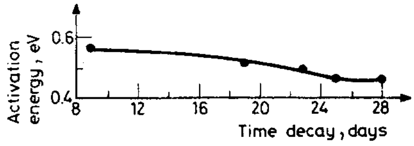

Fig. 4 Effect of time decay (days) on the activation energy (eV)

$$I_c = I_0 e^{-\Delta E/kT} \tag{3}$$

where ΔE is the activation energy for donors or traps, and

$$I_0 = q\mu N_d \frac{V}{d} A \tag{4}$$

where q is the electronic charge, μ is the mobility, N_d is the impurity density, V is the bias voltage, d is the effective electrode separation and A is the effective area.

A plot of $\log I$ againts temperature $(1000/T)$ is shown in Fig. 3. An increasing current passed through the irradiated samples until saturation was attained. This increase in conductivity is due to the decrease of the activation energy of the current carriers accompanied by an increase of the radiation-induced current carriers, as in Fig. 4.

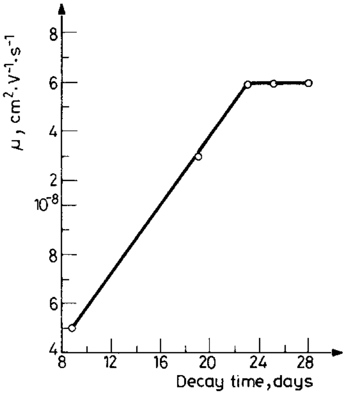

Fig. 5 Dependence of mobility μ on the decay time (days)

The mobility was estimated and the results are shown in Fig. 5. A linear increase was noted; it was accompanied by an increased conductivity to attain saturation, constancy being reached after a decay time of 24 days. This constancy could be correlated with the establishment of the equilibrium state between the annihilation and formation of radiation-induced defects. This may leave behind the gamma-ray damage acting as barrier energy and thus an opposing current flows through the specimen.

Since the present barium zirconate ceramics exhibit a hole conduction mechanism (p-type, as confirmed from a rapid preliminary test for the direction of the galvanometer deflection, using a thermoelectric power circuit), in accordance with previous investigators [18–20] the following equations are equally valid, leading to a suggested theory for the mechanism of gamma-radiation damage of the interaction of γ-rays with barium zirconate ceramic:

(1) In the absence of traps, if radiation falling on the detector produces f ion pairs per second per unit volume, the increase n in the density of free electrons when equilibrium is reached is

$$n = f\tau \tag{5}$$

where τ is the average lifetime of a free electron between production and recombination. This increase in carrier density increases the electrical conductivity σ as follows:

$$\sigma = ne\mu = f\tau e\mu \tag{6}$$

where μ is the electronic mobility and e the electronic charge. Thus, for a maximum change in conductivity, i.e. maximum sensitivity, the product of mobility and lifetime should be as large as possible.

In a pure material with a negligible population of electron traps, recombination occurs directly between vacant holes and free electrons. If no traps are present, but only hole recombination centres, the time t for the current to decay to half its initial value is the carrier lifetime (τ). However, if traps are present, t is increased by the slow thermal release of electrons from traps after the radiation has ceased. The rate of release depends upon the depth of the traps and the temperature of the material. At low dose rates, where $m \gg n$, the time between ionization and recombination is increased by the factor m/n, and t is correspondingly increased because of trapping.

In conclusion, for irradiation with ^{60}Coγ-rays, the Compton effect has the largest cross-section [21] except for materials with very high atomic number and, moreover, the number of atoms displaced per cm^3 per s is a maximum for the very light elements and diminishes [22] up to around atomic weight 125. Irradiation with these rays therefore excludes the possibility of displacement of barium (atomic weight 137.34) by the Compton electrons. Photoelectric and pair production events do not appear to be important in this case [22]. Of the other two mechanisms for displacement production, viz. the Seitz [23] and the Varley [24] mechanisms, the former assumes the discharge of energy into the lattice at irregularities producing local hot spots where the energy available is of the order of 10 eV, but this would produce decomposition rather than displacement of the ZrO_3^{2-} molecular ions. The mechanism of Varley [24] concerns multiple ionization of the anion, but this mechanism will be effective only if the multiply charged anion is stable, as in the case of atomic anions. For molecular anions, as in the present investigations, multiple ionization will generally lead to decomposition. There is, however, the possibility of a cation being ejected to an interstitial position as a result of the coulombic repulsion between it and the momentarily multiply ionized anion, especially since the cations have a greater freedom of movement than the molecular anions [25]. Besides displacement, there occur excitation and ionization of molecular anions produced by chemical damage in the solid state. Thus, upon exposure of barium zirconate to γ-rays, apart from trapped electrons and holes, there will be atoms, radicals and ions in interstitial positions, the fragments bearing the same charge as the parent ion. Over the induction period the point defects anneal out and the energy released at the site of recombination results in the formation of decomposition nuclei [25] in addition to those induced upon irradiation. Consequently, the rate of the linear reaction is higher following irradiation (Fig. 5) since, as has already been said, the surface reaction occurring in this stage depends on the total number of decomposition nuclei existing at the commencement of the reaction.

References

1 E. A. Wood, Acta Cryst., 4 (1951) 353.
2 A. Slvova and N. N. Feodosev, Zh. Fiz. Khim., 38 (1) (1964) 28.
3 H. Granicher, Helv. Phys. Acta, 24 (1959) 619.
4 W. D. Kingery, Introduction to Ceramics, Wiley, New York, 1960.
5 G. Tamman, Z. Anorg. Chem., 21 (1925) 149.
6 A. M. Abd El-Rahim. M. K. El-Nimr, A. Tawfik, M. M. Abou Sekkina and D. M. Hemeda, Proceedings of the Mathematical and Physical Society of Egypt, 49 (1980) 155.
7 J. Rudolph, Z. Naturforsch, 14a, 8 (1959) 727.
8 F. H. Attix, Radiation Dosimetry, Second Edition, Academic Press, N.Y., San Francisco, London, 1966,p. 291.
9 F. H. Attix and W. C. Roesch, Radiation Dosimetry, Second Ed. Academic Press, N.Y., San Francisco, London, 1966, p. 293.
10 L. E. Hollander, Nucleonics, 14 (1956) 68.
11 B. A. Turner, D. H. Mash and J. F. Fomler, Phys. Med. Biol. 8 (1963) 439.
12 M. M. Abou Sekkina, N. Hamame and S. A. Abou El-Enein, Isotopenpraxis, 19 (1983) 163.
13 M. M. Abou Sekkina, E. M. H. Ibrahim and S. B. Hanna, Ceramic Research Bulletin, 26 (1979) 1.
14 E. M. H. Ibrahim, S. B. Hanna and M. M. Abou Sekkina, Arab J. of Nucl. Science and Applications, 11 (1978) 99.
15 M. J. Smith, J. Appl. Phys., 34 (1963) 2879.
16 P. W. Levy, Misc. Publ. Nat. Bur. Stand. (U.S.A.) No. 7 (1966) 21.
17 M. M. Abou Sekkina and A. Tawfik, Indian J. Phys., 54A, 44 (1980) India.
18 A. Rose, Phys. Rev., 97 (1955) 1538.
19 J. F. Fomler, Phys. Med. Biol., 3 (1959) 395.
20 C. G. Clayton and J. B. Whittaker, Nucleonics, 21 (4) (1963) 60.
21 R. D. Evans, The Atomic Nucleus, McGraw Hill, New York, 1967, 211.
22 G. J. Dienes and G. H. Vineyard, Radiation Effects in Solids, Interscience, New York, 1957, p. 129.
23 F. Seite, Rev. Mod. Phys., 26 (7) (1954) 7.
24 J. H. O. Verley, Nature, 174 (1945) 886.
25 E. G. Prout and P. J. Herley, J. Phys. Chem., 66 (1962) 961.

Zusammenfassung — Gut gesinterte Bariumzirkonatkörper wurden hergestellt und identifiziert. An diesen Proben wurden umfassende Messungen vorgenommen, einschließlich röntgendiffraktometrische und die der elektrischen Gleichstromleitfähigkeit in Abhängigkeit von der Temperatur vor und nach Bestrahlung mit Gamma-Strahlen und in Abhängigkeit von der nach der Bestrahlung vergangenen Zeit (Abklingzeit). Die Kurve des Widerstandes in Abhängigkeit von der Temperatur weist bei etwa 60° eine abrupte Änderung in entgegengesetzte Richtung auf, was auf einen wahrscheinlichen Übergang des halbleitungsmechanismus vom *n*- zum *p*-Typ hinweist. Die in Einzelheiten diskutierten Ergebnisse sind miteinander in Übereinstimmung und werden mit der Wirkung der Temperatur und der durch Bestrahlung verursachten Schädigung und Annihilation des Bariumzirkonatgitters in Zusammenhang gebracht.

Резюме — На основе цирконата бария получены и охарактеризованы хорошо спекающиеся образцы керамики. Полученные образцы были подвергнуты обширным исследованиям, включая рентгено-фазовый анализ, измерения *dc*-электропроводности в зависимости от температуры, дозы облучения их гамма-лучами, а также в различные периоды времени (время радиоактивного распада) после удаления образцов из зоны облучения. Кривая температурной зависимости удельного сопротивления показала при температуре около 60° резкий излом в обратное направление, указывая тем самым на возможный $n-p$-переход. Полученные результаты детально обсуждены и скоррелированы с влиянием температуры, действием ионизирующего излучения и радиоактивной аннигиляции на решетку цирконата бария.